

# The Spectrum of Interventional MRI

David Woodrum, M.D., Ph.D.; Setayesh Sotoudehnia Korani, M.D.; Scott Thompson, M.D., Ph.D.

Mayo Clinic, Rochester, MN, USA

## Abstract

Clinical use of magnetic resonance imaging (MRI) for image-guided procedures began in the late 1980s. However, early procedures were limited by tools, in-bore access to the patient, and MR imaging limitations. Interventional MRI (iMRI) offers some natural advantages including superior soft tissue resolution, ease of multiplanar imaging, lack of ionizing radiation, and the ability to re-image the same slice. MRI guidance is particularly advantageous when the pathology can be best or only visualized with MRI. There has been tremendous growth in clinical applications and positive patient outcomes of iMRI over the past three decades, and the community has benefited from close collaboration between interventional radiologists, MR physicists, and MR nurses. There has been tremendous growth in clinical applications of iMRI over the last 35+ years [1]. The purpose of this article is to give a high-level overview of the breadth of interventional MRI.

## Introduction

Shortly after the introduction of clinical diagnostic magnetic resonance imaging (MRI) in the 1980s, diagnostic and interventional radiologists recognized the superior soft tissue contrast of MRI and began to explore the use of MRI guidance during interventional procedures, particularly for head and neck lesions [2–4]. However, early applications of interventional MRI (iMRI) were limited due to the lack of dedicated iMRI magnets, pulse sequences, procedural suites, and equipment. Over the next three decades, significant advancements in iMRI-conditional technology coupled with developments in dedicated iMRI procedural

suites enabled significant growth and development of clinical body iMRI applications including aspiration, localization, biopsy, and ablation [5, 6]. MRI offers significant advantages including: superior soft tissue contrast and anatomic detail, leading to increased lesion conspicuity; ease of multiplanar imaging; multiparametric imaging capabilities; lack of ionizing radiation; the ability to monitor effects of treatment in near real time; and the ability to re-image the same slice [7, 8].

With the growth of dedicated clinical iMRI services, safety considerations in the iMRI environment have become paramount [9, 10]. Moreover, systematic physics and clinical safety testing have led to the safe use of previously MR-conditional and unsafe devices in the MR environment, further enabling expansion of clinical body iMRI applications [9, 11–13]. Likewise, with the growth of dedicated iMRI magnets, various MR pulse sequences have been optimized with tradeoffs between image acquisition speed, signal-to-noise ratio (SNR), and spatial and contrast resolution [14, 15].

Additionally in this time period, there has been tremendous development of commercially available MR-conditional needles, and biopsy and ablation devices, which has further enabled the growth of body iMRI applications [10, 16]. Currently, there are a variety of devices approved by the Food and Drug Administration (FDA) for performing MRI-guided and monitored cryoablation, laser ablation, microwave ablation (MWA), radiofrequency ablation (RFA), and focused ultrasound (MRgFUS). Current iMRI applications include localization, biopsy, and sclerotherapy of lesions with poor soft tissue contrast on other imaging modalities, and thermal ablation for benign and malignant neoplastic processes.

## Clinical applications of body interventional MRI

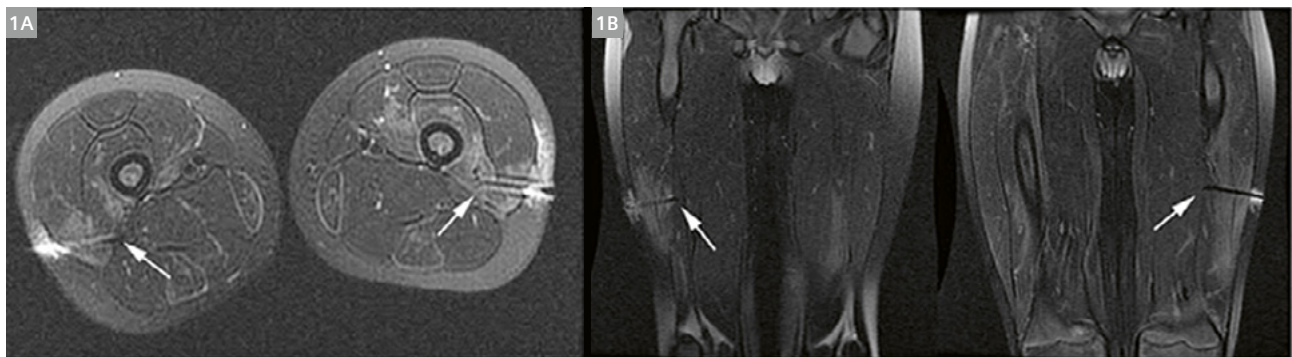
There has been tremendous growth in applications of body iMRI, including localization, drainage, biopsy, and sclerotherapy of lesions poorly visualized with ultrasound (US) or computed tomography (CT) [7, 8, 16–18]. This review focuses on many, but not all, iMRI applications as these continue to grow.

### Localization

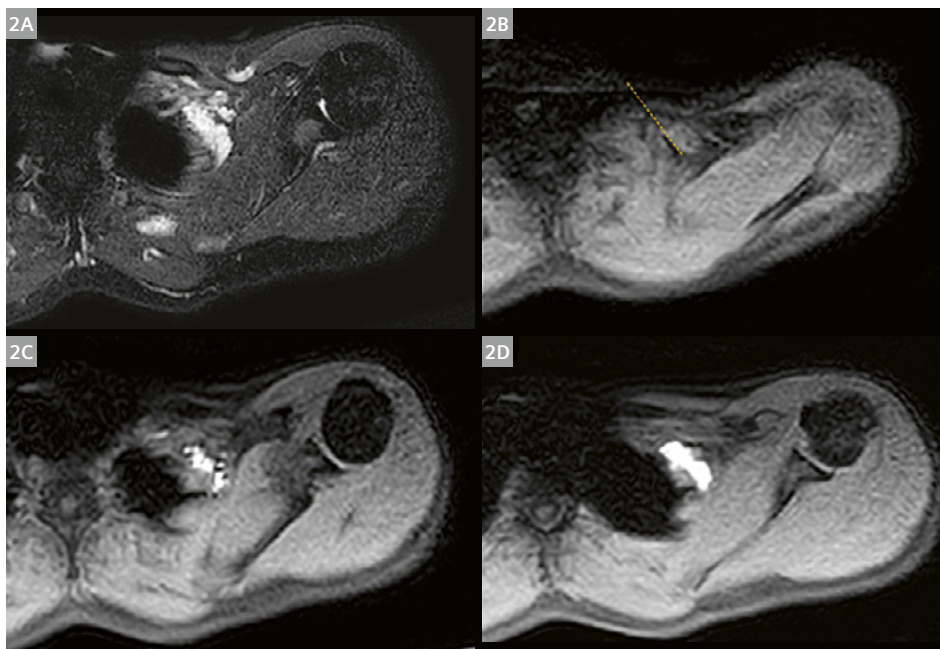
Soft tissue pathology with poor soft tissue contrast on US or CT may be particularly amenable to MRI-guided wire localization when precise localization of a pathology with a patchy or heterogenous distribution is needed prior to targeted surgical biopsy. Examples include intramuscular lymphoma and juvenile dermatomyositis (Fig. 1) [19, 20].

### Sclerotherapy

Traditionally, percutaneous sclerotherapy of venous malformations has been performed with a combination of US and fluoroscopic guidance. However, when venous malformations are poorly conspicuous on US, MRI guidance for needle placement prior to sclerotherapy may be utilized, particularly given the inherent high T2-weighted signal within most venous malformations (Fig. 2). Prior studies have shown that MRI-guided percutaneous sclerotherapy is safe, technically feasible, and effective in the treatment of peripheral soft tissue venous malformations at both 1.5T and 3T [21, 22].



**1** MRI of the needle position within the high T2 signal in the vastus lateralis. **(1A)** Axial and **(1B)** coronal with the localizing wire in place and subsequent surgical biopsy confirming juvenile dermatomyositis [40].



**2** **(2A)** T2 with fat saturation demonstrates a bright slow-flow vascular malformation. **(2B)** shows a 22Ga ITP needle placed into the vascular malformation. **(2C)** demonstrates injection of dilute 1:10 gadolinium into the vascular malformation confirming the intra-luminal position. **(2D)** demonstrates injection of a gadolinium and bleomycin mixture into the lesion to perform sclerotherapy. (Unpublished images)

### Biopsy

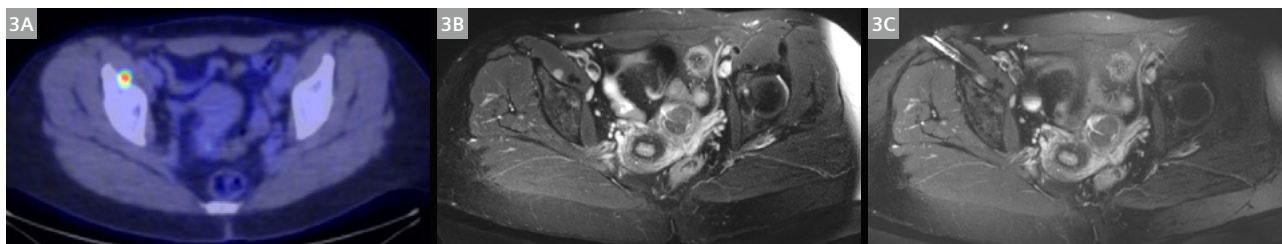
Similar to lesion localization, soft tissue masses with poor soft tissue contrast on US or CT may be suitable for MRI-guided biopsy. This may be performed using freehand, US-assisted or guidance-grid techniques depending on lesion location and organ movement [8, 16, 18, 23]. Prostate and seminal vesicle biopsy via a transperineal approach with a guidance grid is well suited for MRI-guided biopsy [23–25]. Small liver or soft tissue lesions (Fig. 3) seen on diagnostic MRI and positron emission tomography (PET) that cannot be localized by grayscale, color doppler, or contrast-enhanced US, US fusion, or CT are excellent candidates for MRI-guided freehand biopsy. For patients with prior non-diagnostic biopsies of small or technically difficult lesions, consideration can be given to having an on-site cytopathologist for immediate review of the diagnostic adequacy of the biopsy specimen.

### Ablation

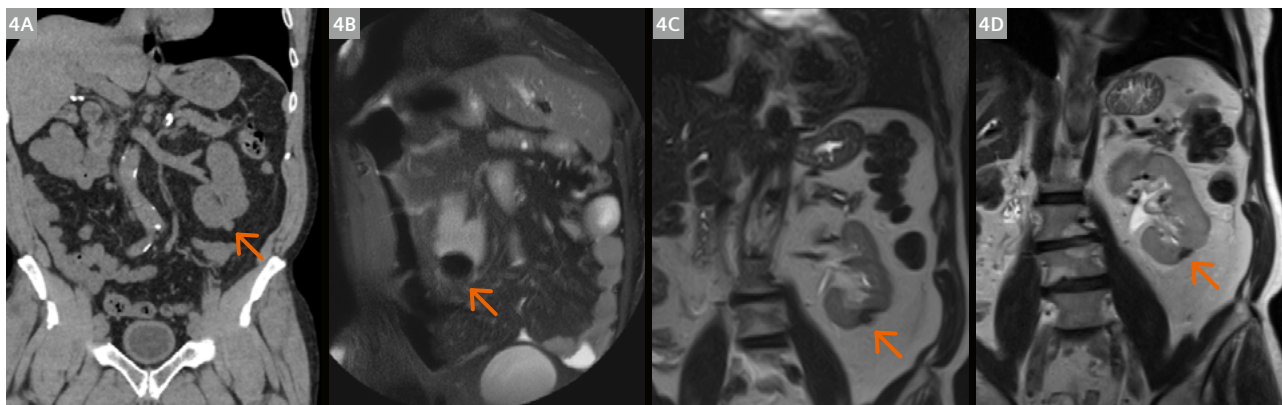
Image-guided percutaneous thermal ablation with MRI is enhanced with more precise lesion visualization and the ability to monitor ablation temperature: either heat or cold. While US, and to a lesser extent CT, can provide some real-time ablation monitoring, MRI has superior soft tissue contrast and, together with MR thermometry, offers a unique feature for monitoring the ablation procedure.

### Kidney

Ablation of renal neoplasms is most commonly performed under US and/or CT guidance using cryoablation, RFA or MWA [26, 27]. However, MRI-guided cryoablation has been shown to be safe and effective for treatment of small renal neoplasms [28]. In our practice, MRI-guided cryoablation is reserved for ablation of renal neoplasms that are intra-parenchymal or endophytic and poorly visualized on US or non-contrast CT (Fig. 4).



**3** MRI-guided muscle lesion biopsy to determine benign versus malignant. **(3A)** shows an axial fluorodeoxyglucose (FDG) PET-CT image demonstrating a lesion with increased activity in the right iliopsoas muscle. CT-guided biopsy was unsuccessful. **(3B)** demonstrates a T2-weighted MR lesion in the same location as the abnormal PET activity. **(3C)** demonstrates an 18Ga ITP biopsy needle through the lesion. (Unpublished images)



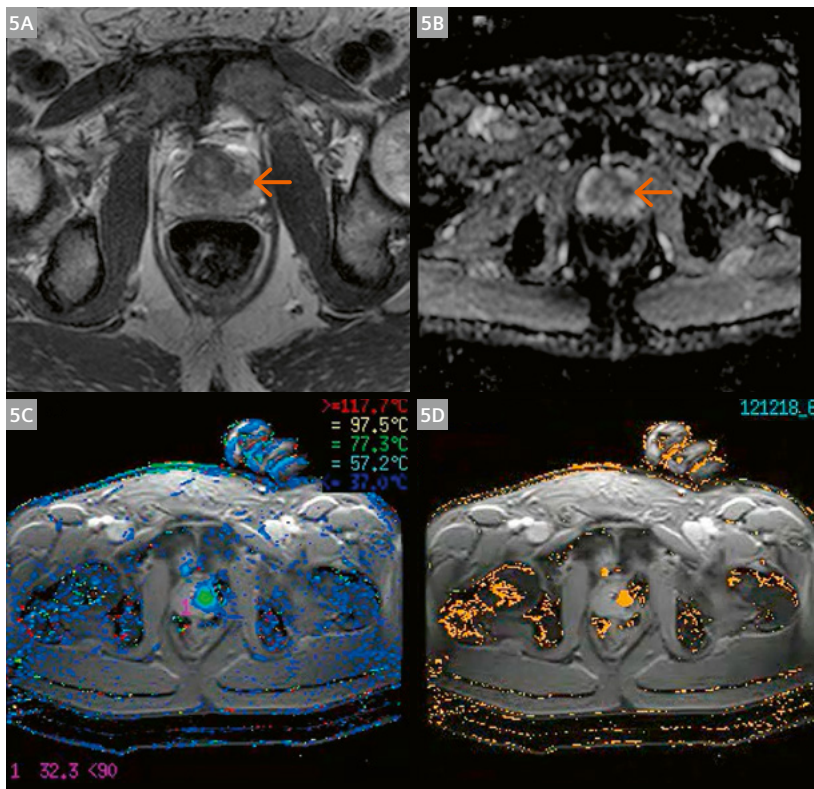
**4** MRI-guided renal mass ablation for a 65-year-old man with a history of right kidney resection for renal cell carcinoma and development of a new left lower pole renal mass. **(4A)** shows a non-contrast CT image demonstrating a tiny mass on the lower pole of the left kidney. **(4B)** demonstrates T2-weighted MR images showing the iceball encompassing the tiny nodule. **(4C)** shows T2-weighted images three months post-ablation. **(4D)** shows T2-weighted images two years post-ablation. (Unpublished images)

### Prostate and seminal vesicles

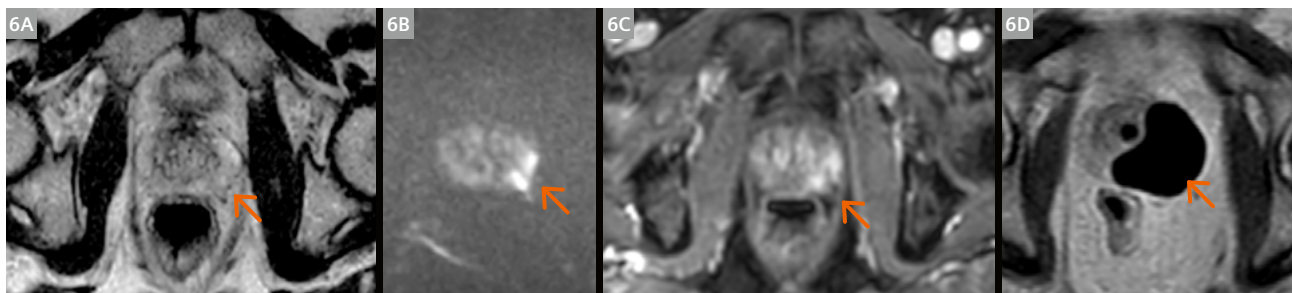
MRI-guided laser ablation of the prostate with MR thermometry in a 64-year-old man with rising prostate specific antigen (PSA) and biopsy-positive Gleason 7 (4+3) disease in the left mid prostate: MRI-guided thermometry allows continuous monitoring of the ablation heating during treatment (Fig. 5).

MRI-guided focal cryoablation of the prostate for Gleason 7 (3+4) disease in the left anterior prostate: Ice ball monitoring is achieved with a balanced HASTE updating every 10–20 seconds (Fig. 6).

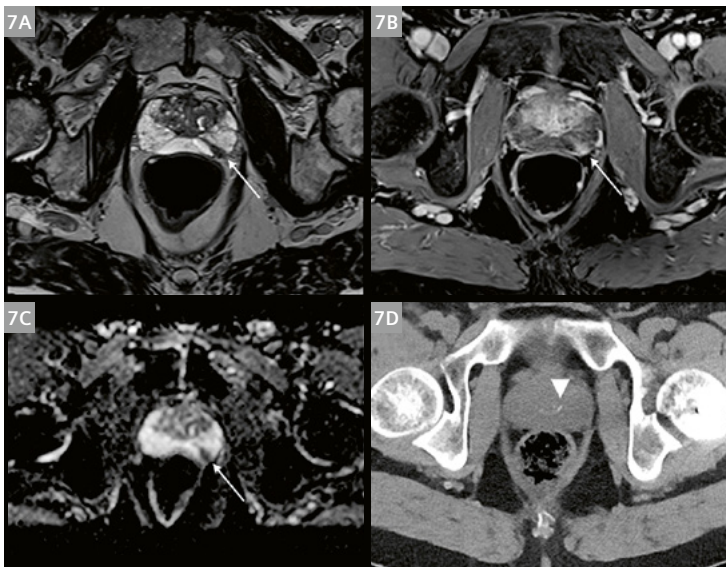
MRI-guided focused transurethral ultrasound ablation (TULSA) of the prostate for Gleason 7 disease in the left posterior prostate: The TULSA treatment device (TULSA-PRO, Profound Medical Corp., Mississauga, Canada) was placed over the wire into the urethra and positioned with the transducers in the prostatic tissue. During treatment, the MR temperature mapping is used to guide and control the treatment frequency and the power, which is monitored continuously.



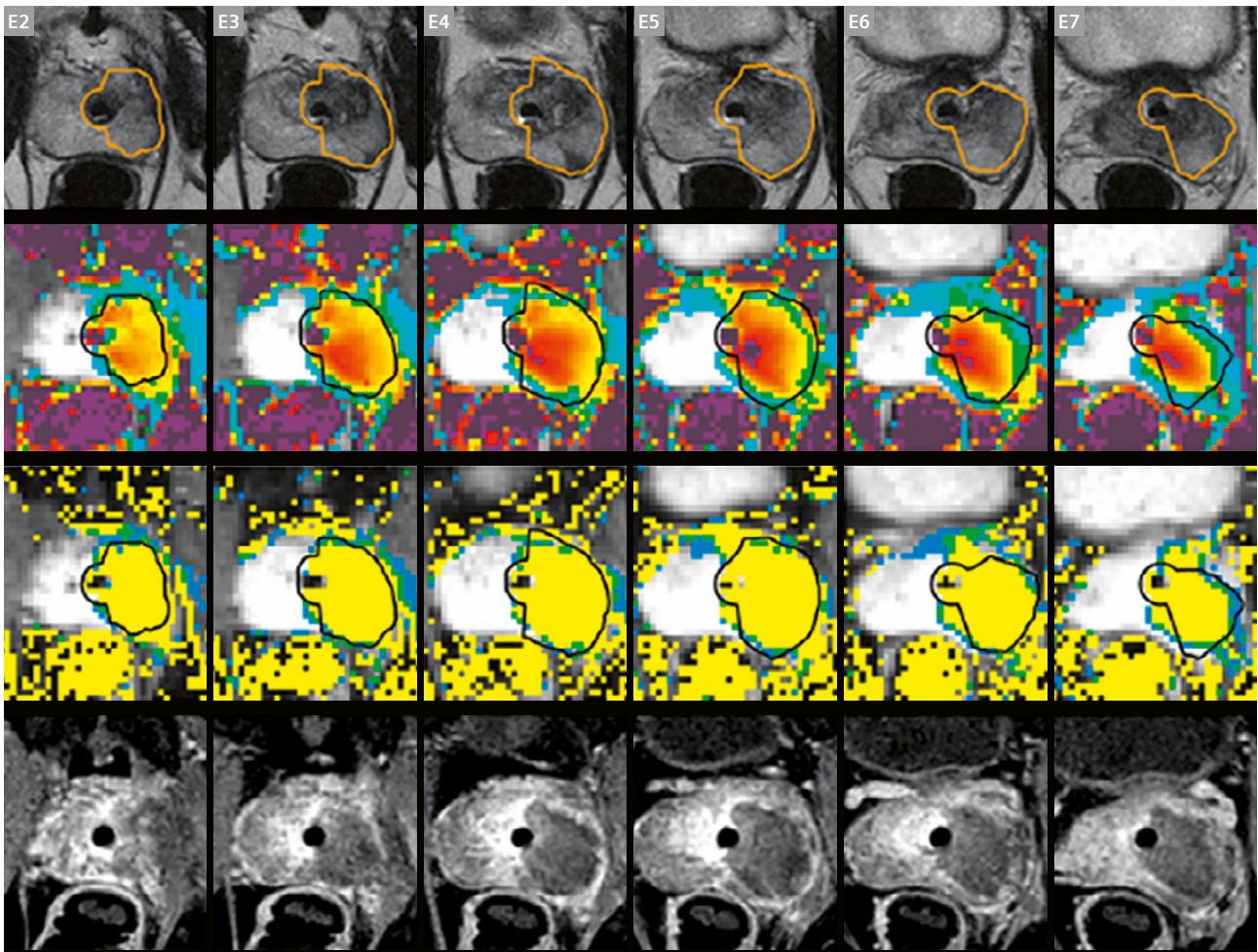
**5** (5A) demonstrates T2-weighted imaging of the prostate showing a lesion in the left prostate. (5B) shows the ADC map demonstrating the restricted diffusion in the left prostate lesion. (5C) is the phase image during MR thermometry demonstrating heating in the left prostate. (5D) is the calculated damage map using time and temperature inputs into an Arrhenius equation. (Unpublished images)



**6** (6A) shows a T2-weighted image demonstrating decreased signal in the left posterior prostate (orange arrow). (6B) demonstrates restricted diffusion in this same area (orange arrow). (6C) demonstrates Gadolinium enhancement in this same area (orange arrow). (6D) demonstrates maximal ice ball formation encompassing the lesion (orange arrow). (Unpublished images)



**7** Pre-treatment workup for the MRI-guided TULSA for prostate cancer. (7A) demonstrates T2 abnormality in the left posterior peripheral zone of the prostate (white arrow). (7B) demonstrates hyperenhancement in a similar location after gadolinium (white arrow). (7C) demonstrates restricted diffusion in the ADC map for the lesion (white arrow). (7D) demonstrates some very tiny calcifications, which can be worked around with the TULSA device (white arrowhead). (Unpublished data)

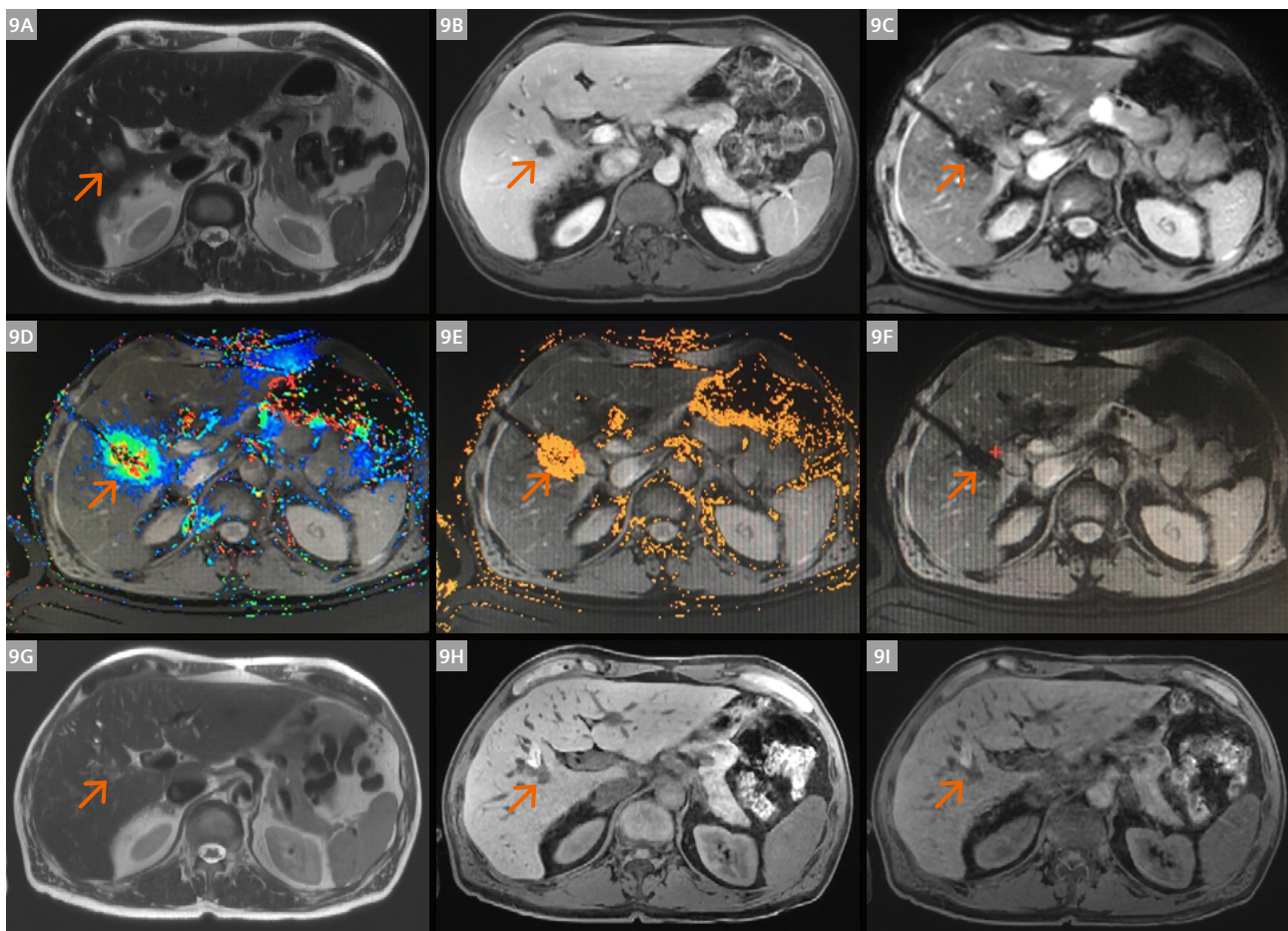


**8** Summary images from the MRI-guided TULSA treatment. The first row shows the T2-weighted anatomic images corresponding to the location of the individual US transducers from E2–E7. The second row shows the maximal heat delivered by each US transducer at each level. The third row shows the calculated damage map based on the Arrhenius equation. The fourth row shows the postgadolinium images after the ablation, confirming the treatment zone at each level. (Unpublished data)

### Hepatobiliary

Image-guided thermal ablation is considered a curative-intent treatment for very early or early stage hepatocellular carcinoma (HCC) [29]. Additionally, thermal ablation is used for treatment of a wide range of metastases to the liver, particularly colorectal liver metastases (CRLM) [30]. Historically, US and CT were the most common imaging modalities used for guidance and monitoring during hepatic radiofrequency or microwave ablation [31, 35]. However, in recent years, MRI-guided thermal ablation

including RFA, MWA (Fig. 9), laser ablation, and cryoablation have emerged as safe and effective treatment options, particularly when the liver lesion is best visualized by MRI. We have found MRI guidance and monitoring for ablation particularly useful for small hepatic tumors that are poorly visualized by ultrasound, and for tumors deep in the liver such as in the caudate lobe, high up in the hepatic dome, or adjacent to critical structures such as central bile ducts, stomach, or colon, where monitoring of the ablation zone is critical.



**9** MRI-guided microwave ablation in a 72-year-old male for metastatic prostate cancer to the liver with central lesion. (9A) is the T2 weighted image demonstrating a small central lesion (orange arrow). (9B) shows the post-gadolinium image demonstrating delayed enhancement to the remaining liver typical of prostate cancer mets (orange arrow). (9C) demonstrates placement of the microwave antennae using a combination of US/MRI guidance (orange arrow). (9D) (phase imaging), (9E) (estimated damage map), and (9F) (T1 anatomic imaging) are from the temperature mapping proton resonance frequency imaging during the ablation. (9D) demonstrates the active temperature rise from the ablation (orange arrow). (9E) shows the damage map based on time and temperature change measurements using the Arrhenius equation (orange arrow). Followup MRI at three months post-ablation with (9G) (T2-weighted images), (9H) (pre-contrast T1 images), and (9I) (post-gadolinium images) demonstrating significant decrease in size since treatment consistent with evolving ablation changes. (Unpublished images)

### Musculoskeletal and soft tissue

There has been an increasing role for image-guided thermal ablative therapies in the treatment of musculoskeletal and soft tissue tumors including the use of MRI guidance [36–38]. MRgFUS and cryoablation are feasible for treatment of focal metastatic disease to the bone. Additionally, several series have reported on the safety and effectiveness of percutaneous ablation for treatment of extra-abdominal desmoid tumors [39–41]. MRI-guided ablation is particularly beneficial when desmoid tumors are in close proximity to critical structures such as hollow viscus or nerves. Lastly, in patients with soft tissue oligometastatic disease, MRI-guided cryoablation offers a minimally invasive palliative treatment option [42, 43].

### Peripheral soft tissue vascular anomalies

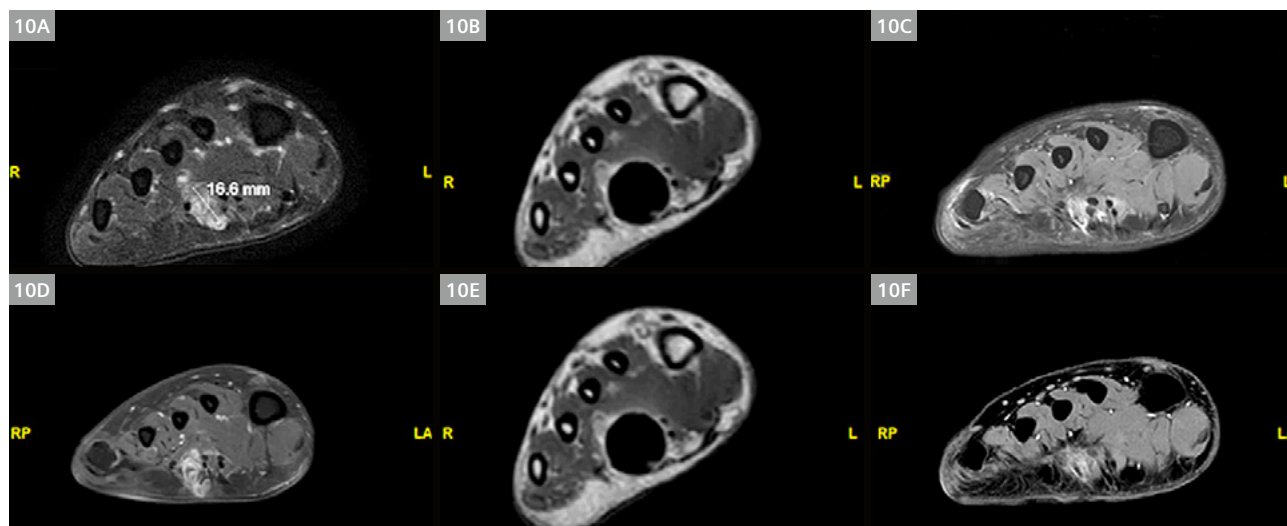
Peripheral soft tissue vascular anomalies (VA) include vascular tumors and vascular malformations. While percutaneous image-guided sclerotherapy and embolization are considered first-line treatments for symptomatic VA depending on size, location, and flow characteristics, emerging evidence suggests that MRI-guided laser ablation and cryoablation (Fig. 10) are safe and effective for treatment of symptomatic peripheral soft tissue VA [44–46]. In our practice, the most common vascular anomalies we treat with MRI-guided ablation include both pediatric and adult focal slow-flow venous or venolymphatic malformations, and focal vascular tumors, most commonly in the trunk or extremities. Less commonly, we have treated small focal high-flow arteriovenous malformations (AVMs)

with MRI-guided ablation and a tourniquet proximal to the site of ablation to decrease the high flow, and focal cervicofacial slow-flow venous malformations.

### Conclusions and future directions

Significant advancements in iMRI magnets, technology, and devices over the last three decades have enabled rapid growth of clinical body iMRI applications including lesion localization, biopsy, drainage, sclerotherapy, and ablation. Building a successful clinical iMRI practice requires

1. multidisciplinary collaboration and teamwork, including interventional and diagnostic radiologists, clinicians, MR physicists, technologists and nurses, anesthesiologists and nurse anesthetists, administrators and industry partners,
2. investment in personnel, space, equipment, and resources,
3. education of referring clinicians regarding the clinical safety and effectiveness of clinical body iMRI applications, particularly as a problem-solving tool when other image-guided procedures have failed or are deemed not technically feasible. Safety in the iMRI environment is paramount and requires close collaboration with MR physicists and MRI safety officers. Ongoing technological and technique advancements such as interventional PET/MRI, advanced navigation systems, and robotics will help interventional radiologists continue to push the frontiers of body iMRI applications in the coming decades [47, 48].



**10** (10A) demonstrates high T2 signal in the plantar aspect of the foot, representing a slow-flow vascular malformation causing significant pain to the patient every day when walking. (10D) demonstrates the gadolinium enhancement within the vascular malformation. (10B) and (10E) demonstrate the ice ball formation during the MRI-guided cryoablation. (10C) represents the postablation T2 signal change, which usually decreases significantly. (10F) represents the postablation gadolinium lack of enhancement consistent with treatment and no flow. (Unpublished images)

## References

- 1 Thompson SM, Gorny KR, Koepsel EMK, Welch BT, Mynderse L, Lu A, et al. Body Interventional MRI for Diagnostic and Interventional Radiologists: Current Practice and Future Prospects. *Radiographics*. 2021;41(6):1785–801.
- 2 Mueller PR, Stark DD, Simeone JF, Saini S, Butch RJ, Edelman RR, et al. MR-guided aspiration biopsy: needle design and clinical trials. *Radiology*. 1986;161(3):605–9.
- 3 Lufkin R, Teresi L, Chiu L, Hanafee W. A technique for MR-guided needle placement. *AJR Am J Roentgenol*. 1988;151(1):193–6.
- 4 Duckwiler G, Lufkin RB, Teresi L, Spickler E, Dion J, Vinuela F, et al. Head and neck lesions: MR-guided aspiration biopsy. *Radiology*. 1989;170(2):519–22.
- 5 Sedaghat F, Tuncali K. Enabling Technology for MRI-Guided Intervention. *Top Magn Reson Imaging*. 2018;27(1):5–8.
- 6 Busse H, Kahn T, Moche M. Techniques for Interventional MRI Guidance in Closed-Bore Systems. *Top Magn Reson Imaging*. 2018;27(1):9–18.
- 7 Sequeiros RB, Ojala R, Kariniemi J, Perala J, Niinimäki J, Reinikainen H, et al. MR-guided interventional procedures: a review. *Acta Radiol*. 2005;46(6):576–86.
- 8 Weiss CR, Nour SG, Lewin JS. MR-guided biopsy: a review of current techniques and applications. *J Magn Reson Imaging*. 2008;27(2):311–25.
- 9 White MJ, Thornton JS, Hawkes DJ, Hill DLG, Kitchen N, Mancini L, et al. Design, operation, and safety of single-room interventional MRI suites: practical experience from two centers. *J Magn Reson Imaging*. 2015;41(1):34–43.
- 10 Nour SG, Lewin JS. Creating a Clinical Interventional MRI Service. *Top Magn Reson Imaging*. 2018;27(1):25–31.
- 11 Lu A, Woodrum DA, Felmler JP, Favazza CP, Gorny KR. Improved MR-thermometry during hepatic microwave ablation by correcting for intermittent electromagnetic interference artifacts. *Phys Med*. 2020;71:100–107.
- 12 Gorny KR, Favazza CP, Lu A, Felmler JP, Hangiandreou NJ, Browne JE, et al. Practical implementation of robust MR-thermometry during clinical MR-guided microwave ablations in the liver at 1.5 T. *Phys Med*. 2019;67:91–99.
- 13 Ma C, Long ZY, Lanners DM, Tradup DJ, Brunquell CL, Felmler JP, et al. Protocol for testing suitability of compact US imaging systems for use inside MRI suites, and application to one commercial US system. *Biomed Phys Eng Expr*. 2016;2(4).
- 14 Yutzey SR, Duerk JL. Pulse sequences and system interfaces for interventional and real-time MRI. *J Magn Reson Imaging*. 2008;27(2):267–75.
- 15 Kahn T, Busse H. *Interventional magnetic resonance imaging*. Heidelberg: Springer; 2012. xvii, pp. 496.
- 16 Kaye EA, Granlund KL, Morris EA, Maybody M, Solomon SB. Closed-Bore Interventional MRI: Percutaneous Biopsies and Ablations. *AJR Am J Roentgenol*. 2015;205(4):W400–10.
- 17 Lewin JS, Nour SG, Duerk JL. Magnetic resonance image-guided biopsy and aspiration. *Top Magn Reson Imaging*. 2000;11(3):173–83.
- 18 Nour SG, Lewin JS. Percutaneous biopsy from blinded to MR guided: an update on current techniques and applications. *Magn Reson Imaging Clin N Am*. 2005;13(3):441–64.
- 19 Thompson SM, Gorny KR, Jondal DE, Rech KL, Mardini S, Woodrum DA. MRI-guided Wire Localization Surgical Biopsy in an Adolescent Patient with a Difficult to Diagnose Case of Lymphoma. *Cardiovasc Intervent Radiol*. 2017;40(1):135–138.
- 20 Tuen VC, Zingula SN, Moir C, Reed AM, Matsumoto JM, Woodrum DA. MRI guided wire localization muscle biopsy in a child with juvenile dermatomyositis. *Pediatr Rheumatol Online J*. 2013;11(1):15.
- 21 O'Mara DM, Berges AJ, Fritz J, Weiss CR. MRI-guided percutaneous sclerotherapy of venous malformations: initial clinical experience using a 3T MRI system. *Clin Imaging*. 2020;65:8–14.
- 22 Andreisek G, Nanz D, Weishaupt D, Pfammatter T. MR imaging-guided percutaneous sclerotherapy of peripheral venous malformations with a clinical 1.5-T unit: a pilot study. *J Vasc Interv Radiol*. 2009;20(7):879–87.
- 23 Woodrum DA, Gorny KR, Greenwood B, Mynderse LA. MRI-Guided Prostate Biopsy of Native and Recurrent Prostate Cancer. *Semin Intervent Radiol*. 2016;33(3):196–205.
- 24 Woodrum DA, Gorny KR, Mynderse LA. MR-Guided Prostate Interventions. *Top Magn Reson Imaging*. 2018;27(3):141–151.
- 25 Woodrum DA, Kawashima A, Gorny KR, Mynderse LA. Targeted prostate biopsy and MR-guided therapy for prostate cancer. *Abdom Radiol (NY)*. 2016;41(5):877–88.
- 26 Atwell TD, Schmitz GD, Boorjian SA, Mandrekar J, Kurup AN, Weisbrod AJ, et al. Percutaneous ablation of renal masses measuring 3.0 cm and smaller: comparative local control and complications after radiofrequency ablation and cryoablation. *AJR Am J Roentgenol*. 2013;200(2):461–6.
- 27 Thompson SM, Schmitz JJ, Thompson RH, Weisbrod AJ, Welch BT, Viers BR, et al. Introduction of Microwave Ablation Into a Renal Ablation Practice: Valuable Lessons Learned. *AJR Am J Roentgenol*. 2018;211(6):1381–1389.
- 28 Cazzato RL, De Marini P, Leonard-Lorant I, Leclerc L, Auloge P, Tricard T, et al. Safety and Oncologic Outcomes of Magnetic Resonance Imaging-Guided Cryoablation of Renal Cell Carcinoma: A 10-Year Single-Center Experience. *Invest Radiol*. 2021;56(3):153–162.
- 29 Weinstein JL, Ahmed M. Percutaneous Thermal Ablation for Hepatocellular Carcinoma. *Semin Intervent Radiol*. 2020;37(5):527–536.
- 30 Ruers T, Van Coevorden F, Punt CJ, Pierie JE, Borel-Rinkes I, Ledermann JA, et al. Local Treatment of Unresectable Colorectal Liver Metastases: Results of a Randomized Phase II Trial. *J Natl Cancer Inst*. 2017;109(9):djj015.
- 31 Yang N, Gong J, Yao L, Wang C, Chen J, Liu J, et al. Magnetic resonance imaging-guided microwave ablation of hepatic malignancies: Feasibility, efficacy, safety, and follow-up. *J Cancer Res Ther*. 2020;16(5):1151–1156.
- 32 Xiang J, Liu M, Lu R, Wang L, Xu Y, He X, et al. Magnetic resonance-guided ablation of liver tumors: A systematic review and pooled analysis. *J Cancer Res Ther*. 2020;16(5):1093–1099.
- 33 Winkelmann MT, Gohla G, Kubler J, Weiss J, Clasen S, Nikolaou K, et al. MR-Guided High-Power Microwave Ablation in Hepatic Malignancies: Initial Results in Clinical Routine. *Cardiovasc Intervent Radiol*. 2020;43(11):1631–1638.
- 34 Weiss J, Winkelmann MT, Gohla G, Kubler J, Clasen S, Nikolaou K, et al. MR-guided microwave ablation in hepatic malignancies: clinical experiences from 50 procedures. *Int J Hyperthermia*. 2020;37(1):349–355.
- 35 Chen J, Lin Z, Lin Q, Lin R, Yan Y, Chen J. Percutaneous radiofrequency ablation for small hepatocellular carcinoma in hepatic dome under MR-guidance: clinical safety and efficacy. *Int J Hyperthermia*. 2020;37(1):192–201.
- 36 Ahrar K, Sabir SH, Yevich SM, Sheth RA, Ahrar JU, Tam AL, et al. MRI-Guided Interventions in Musculoskeletal System. *Top Magn Reson Imaging*. 2018;27(3):129–139.
- 37 Nour SG, Monson DK. MRI-guided musculoskeletal soft tissue interventions. *Top Magn Reson Imaging*. 2011;22(4):197–205.
- 38 Kurup AN, Callstrom MR. Increasing Role of Image-Guided Ablation in the Treatment of Musculoskeletal Tumors. *Cancer J*. 2016;22(6):401–410.

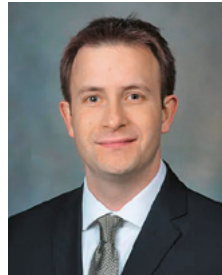
- 39 Griffin MO, Kulkarni NM, O'Connor SD, Sudakoff GS, Lea WB, Tutton SM. Magnetic Resonance-Guided Focused Ultrasound: A Brief Review With Emphasis on the Treatment of Extra-abdominal Desmoid Tumors. *Ultrasound Q*. 2019;35(4):346–354.
- 40 Havez M, Lippa N, Al-Ammari S, Kind M, Stoeckle E, Italiano A, et al. Percutaneous image-guided cryoablation in inoperable extra-abdominal desmoid tumors: a study of tolerability and efficacy. *Cardiovasc Intervent Radiol*. 2014;37(6):1500–6.
- 41 Schmitz JJ, Schmit GD, Atwell TD, Callstrom MR, Kurup AN, Weisbrod AJ, et al. Percutaneous Cryoablation of Extraabdominal Desmoid Tumors: A 10-Year Experience. *AJR Am J Roentgenol*. 2016;207(1):190–5.
- 42 Vaswani D, Wallace AN, Eiswirth PS, Madaelil TP, Chang RO, Tomasian A, et al. Radiographic Local Tumor Control and Pain Palliation of Sarcoma Metastases within the Musculoskeletal System with Percutaneous Thermal Ablation. *Cardiovasc Intervent Radiol*. 2018;41(8):1223–1232.
- 43 McMenomy BP, Kurup AN, Johnson GB, Carter RE, McWilliams RR, Markovic SN, et al. Percutaneous cryoablation of musculoskeletal oligometastatic disease for complete remission. *J Vasc Interv Radiol*. 2013;24(2):207–13.
- 44 Thompson SM, Callstrom MR, McKusick MA, Woodrum DA. Initial Results of Image-Guided Percutaneous Ablation as Second-Line Treatment for Symptomatic Vascular Anomalies. *Cardiovasc Intervent Radiol*. 2015;38(5):1171–8.
- 45 Cornelis FH, Labreze C, Pinsolle V, Le Bras Y, Castermans C, Bader C, et al. Percutaneous Image-Guided Cryoablation as Second-Line Therapy of Soft-Tissue Venous Vascular Malformations of Extremities: A Prospective Study of Safety and 6-Month Efficacy. *Cardiovasc Intervent Radiol*. 2017;40(9):1358–1366.
- 46 Cornelis FH, Marin F, Labreze C, Pinsolle V, Le Bras Y, Midy D, et al. Percutaneous cryoablation of symptomatic venous malformations as a second-line therapeutic option: a five-year single institution experience. *Eur Radiol*. 2017;27(12):5015–5023.
- 47 Reich CM, Sattler B, Jochimsen TH, Unger M, Melzer L, Landgraf L, et al. Practical setting and potential applications of interventions guided by PET/MRI. *Q J Nucl Med Mol Imaging*. 2020;65(1):43–50.
- 48 Hata N, Moreira P, Fischer G. Robotics in MRI-Guided Interventions. *Top Magn Reson Imaging*. 2018;27(1):19–23.

---

## Contact



David Woodrum, M.D., Ph.D.  
Radiology and Vascular Centers  
Mayo Clinic  
200 First St. SW  
Rochester, MN 55905  
USA  
woodrum.david@mayo.edu



Scott M. Thompson, M.D., Ph.D.  
Radiology  
Mayo Clinic  
200 First St. SW  
Rochester, MN 55905  
USA  
Thompson.scott@mayo.edu

---